5430 *Chem. Mater.* **2010,** *22,* 5430–5436
DOI:10.1021/cm100349c

CHEMISTRY OF MATERIALS
Article

Electrodeposition of Copper and Silver Nanowires in Hierarchical Mesoporous Silica/Anodic Alumina Nanostructures

Andreas Keilbach,[†] James Moses,[†,‡] Ralf Köhn,[†,§] Markus Döblinger,[†] and Thomas Bein*[,†]

[†]*Department of Chemistry and Center for NanoScience (CeNS), University of Munich, Butenandtstrasse 5-13 (E), 81377 Munich, Germany,* [‡]*Department of Engineering Science and Mechanics, The Pennsylvania State University, University Park, Pennsylvania 16801, and* [§]*Centre for Free-Electron Laser Science, Notkestrasse 85, 22607 Hamburg, Germany*

Received February 3, 2010. Revised Manuscript Received May 30, 2010

Copper, silver, and tellurium nanowires were electrodeposited into a hierarchical channel structure formed from columnar silica mesophases inside of anodic alumina membranes. The resulting wires were structurally and spectroscopically characterized within the host matrix, in the partially dissolved matrix, and completely removed from the matrix with electron microscopy methods. Plan view images of wires featuring 10 nm diameter within the intact matrix showed the successful replication of the hexagonal arrangement of the columnar mesoporous system. Dissolving only the alumina while leaving the silica mesophase still intact, the long-range organization of the mesoporous system could be visualized. Finally, by completely dissolving the matrix (both alumina and silica), silver wires in the form of bundles of individual wires of about 10 nm diameter could be obtained.

Introduction

During the past decade one-dimensional nanosystems such as nanowires and nanorods have become a burgeoning field of research.[1−3] Several methods have been developed for the synthesis of such structures, including vapor−liquid−solid (VLS) growth[4,5] and template based methods.[6−8] The VLS method is widely used to grow semiconductor nanowires, due to its ability to grow large numbers of highly pure and single-crystalline nanostructures. The growth process involves a liquid catalyst droplet, which adsorbs precursor molecules from the gas phase. While this approach can produce highly crystalline, high aspect ratio nanowires of numerous materials, the wires are typically not ordered and issues such as contamination from the catalyst can limit the scope of this method.[1] In contrast, template-based synthesis offers the generation of a large variety of nanostructures, does not depend on a catalytic process, and can be used for the synthesis of vastly different materials, such as metals,[9] metal oxides,[10] and semiconductors.[11] Template-based synthesis offers a variety of processing methods to incorporate the required growth species into the template host. Among the most popular methods are electrochemistry, sol−gel chemistry, and impregnation techniques.

Track-etched polycarbonate membranes[12,13] and porous anodic aluminum oxide membranes (AAM or AAO)[14,15] are often used as templates, due to their commercial availability and/or relatively easy synthesis of different channel diameters and channel densities. These porous substrates have a channel system running perpendicular to the membrane surface, allowing the synthesis of nanowires with diameters ranging from about 10 to 400 nm. Over the last decades, these channels have been used for the preparation of a wide range of nanomaterials.[16−18] During the synthesis of the AAM templates, the pore size is controlled by the electrolyte and the anodization voltage. By optimizing the parameters, even sub-10-nm tellurium nanowires could be realized.[18] Another elegant way to tailor the pore size to specific values has been demonstrated by using atomic layer deposition to coat the AAM

*Corresponding author. Fax: (+49-89-2180-77622). E-mail: bein@lmu.de.

(1) Cao, G.; Liu, D. *Adv. Colloid Interface Sci.* **2008**, *136*(1−2), 45–64.
(2) Wang, J. *J. Mater. Chem.* **2008**, *18*(34), 4017–4020.
(3) Tian, B.; Kempa, T. J.; Lieber, C. M. *Chem. Soc. Rev.* **2009**, *38*(1), 16–24.
(4) Chan, C. K.; Peng, H.; Liu, G.; McIlwrath, K.; Zhang, X. F.; Huggins, R. A.; Cui, Y. *Nature Nanotechnol.* **2008**, *3*(1), 31–35.
(5) Lu, W.; Lieber, C. M. *J. Phys. D: Appl. Phys.* **2006**, *39*(21), R387–R406.
(6) Chen, M.; Chien, C. L.; Searson, P. C. *Chem. Mater.* **2006**, *18*(6), 1595–1601.
(7) Petkov, N.; Platschek, B.; Morris, M. A.; Holmes, J. D.; Bein, T. *Chem. Mater.* **2007**, *19*(6), 1376–1381.
(8) Singh, A.; Ghosh, A. *J. Phys. Chem. C* **2008**, *112*(10), 3460–3463.
(9) Nielsch, K.; Müller, F.; Li, A.-P.; Gösele, U. *Adv. Mater.* **2000**, *12*(8), 582–586.
(10) Wang, Q.; Wang, G.; Xu, B.; Jie, J.; Han, X.; Li, G.; Li, Q.; Hou, J. G. *Mater. Lett.* **2005**, *59*(11), 1378–1382.
(11) Wang, W.-L.; Wan, C.-C.; Wang, Y.-Y. *J. Phys. Chem. B.* **2006**, *110*, 12974−12980.
(12) Cornelius, T. W.; Brötz, J.; Chtanko, N.; Dobrev, D.; Miehe, G.; Neumann, R.; Molares, M. E. T. *Nanotechnology* **2005**, *16*, S246–S249.
(13) Molares, M. E. T.; Buschmann, V.; Dobrev, D.; Newmann, R.; Scholz, R.; Schuchert, I. U.; Vetter, J. *Adv. Mater.* **2001**, *13*, 62–65.
(14) Birjukovs, P.; Petkov, N.; Xu, J.; Svirksts, J.; Boland, J. J.; Holmes, J. D.; Erts, D. *J. Phys. Chem. C* **2008**, *112*(49), 19680–19685.
(15) Bachmann, J.; Jing, J.; Knez, M.; Barth, S.; Shen, H.; Mathur, S.; Gösele, U.; Nielsch, K. *J. Am. Chem. Soc.* **2007**, *129*(31), 9554–9555.
(16) Martin, C. R. *Chem. Mater.* **1996**, *8*, 1739–1746.
(17) Martin, C. R. *Science* **1994**, *266*(5193), 1961–1966.
(18) Wade, T. L.; Wegrowe, J. E. *Eur. Phys. J. Appl. Phys.* **2005**, *29*(1), 3–22.

Published on Web 09/14/2010

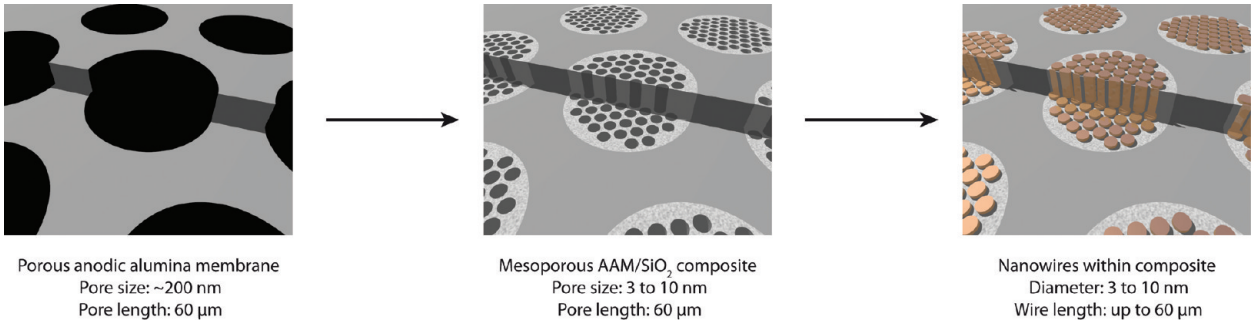

Figure 1. Scheme illustrating the concept of the synthesis of nanowires within hierarchical mesoporous silica/AAM composites. The AAM pores serve as the template for the synthesis of a columnar mesoporous silica structure. This can afterwards be used as the mold for the electrodeposition of nanowires. The AAM/silica mold can be chemically dissolved; thus, free nanowires can be obtained.

pore walls.[19,20] That way pore sizes of about 10 nm were obtained.

Periodic mesoporous silicates with their tunable pore sizes down to about 2 nm could extend this range to even smaller diameters; however, they are usually synthesized in the form of powders or thin films. Due to the random orientation of the channel orientation in powders, there is practically no way to contact the individual particles to an electrode; thus, these systems cannot be used for electrochemical and directed growth of wires within their mesopores. Mesoporous thin films could overcome this issue, but the mesophase system usually aligns parallel to the substrate surface, thus making oriented vertical growth impossible. To overcome this challenge, several methods, such as "nanometer-scale epitaxy"[21] or mesopore alignment by electric field,[22,23] have been reported. Stucky and co-workers have published the synthesis of nanowires by a hierarchical two-mold process, which involves the synthesis of a first mold of an anodic aluminum oxide film that is subsequently filled by a silica mesophase.[24] In that work, the orientation of the mesophase was tuned by changing the diameter of the alumina matrix, resulting in the formation of helical mesopores or isolated mesopore spheres. This mesophase was then used as a template for the replication of the mesopore system by electrodeposition of silver; that way, bundles of spiral-shaped nanowires were obtained.

The orientation of the silica mesophase embedded within the alumina channels can also be controlled by choosing appropriate synthesis conditions during the self-assembly process.[25,26] This makes it possible to extend the mesopore orientation to hexagonal circular, hexagonal columnar, and lamellar arrangements.

Here we report on the synthesis of metal (copper, silver, tellurium) nanowires by electrodeposition within the pores of hexagonal columnar Pluronic P123 triblock copolymer templated mesopores (Figure 1). The mesopore synthesis was carried out using commercially available anodic alumina membranes, thus giving access to high aspect ratios and allowing a reproducible synthesis. By further tuning the synthesis conditions during the evaporation-induced self-assembly process (EISA), mesoporous composites with a high fraction of the hexagonal columnar phase over the hexagonal circular phase have been prepared.[26] Further filling of these mesopores by electrochemical deposition led to the formation of nanowires. Characterization of the wires in plan view orientation (perpendicular view to the membrane surface) without dissolution of the surrounding AAM/silica matrix reveals high filling factors for copper and silver. The wires were further characterized by partial dissolution of the alumina matrix, thus revealing the long-range order of the mesopore channels. Finally, it was possible to obtain individual bundles of silver wires by complete dissolution of the double-mold matrix.

Experimental Details

Synthesis of the Columnar Mesophase System. Whatman Anodiscs (47 mm diameter, nominal pore diameter 0.02 μm, effective pore diameter between 150 and 250 nm) were used as anodic alumina membranes (AAM). The columnar mesopores were synthesized in a manner similar to a previously published procedure.[26] Typically, a prehydrolyzed solution was prepared by mixing 1.8 g (10 mmol) of water, 3.0 g (corresponding to 17 mmol of H_2O and 0.60 mmol of HCl) of hydrochloric acid (0.2 M in water), 3.95 g (85 mmol) of ethanol, and 2.08 g (10 mmol) of tetraethylorthosilicate (TEOS). This solution was then prehydrolyzed at 60 °C for 1 h. To this solution, 0.75 g (0.13 mmol) of Pluronic P123 in 11.86 g (260 mmol) of ethanol and 0.045 g (1 mmol) of lithium chloride were added to induce the formation of the columnar phase. After thorough mixing, 0.75 mL of this solution were cast onto an AAM membrane and dried overnight at 27 °C and 75% relative humidity. The resulting composite membranes were subsequently calcined in air at 500 °C for 5 h, using a heating rate of 0.5 °C per minute.

Electrodeposition. A 100 nm thick gold film was sputtered onto one side of the calcined membranes, serving as the working

(19) Pellin, M. J.; Stair, P. C.; Xiong, G.; Elam, J. W.; Birrell, J.; Curtiss, L.; George, S. M.; Han, C. Y.; Iton, L.; Kung, H.; Kung, M.; Wang, H. H. *Catal. Lett.* **2005**, *102*(3), 127–130.
(20) Xiong, G.; Elam, J. W.; Feng, H.; Han, C. Y.; Wang, H.-H.; Iton, L. E.; Curtiss, L. A.; Pellin, M. J.; Kung, M.; Kung, H.; Stair, P. C. *J. Phys. Chem. B* **2005**, *109*(29), 14059–14063.
(21) Richman, E. K.; Brezesinski, T.; Tolbert, S. H. *Nature Mater.* **2008**, *7*(9), 712–717.
(22) Goux, A.; Etienne, M.; Aubert, E.; Lecomte, C.; Ghanbaja, J.; Walcarius, A. *Chem. Mater.* **2009**, *21*(4), 731–741.
(23) Walcarius, A.; Sibottier, E.; Etienne, M.; Ghanbaja, J. *Nature Mater.* **2007**, *6*(8), 602–608.
(24) Wu, Y.; Cheng, G.; Katsov, K.; Sides, S. W.; Wang, J.; Tang, J.; Fredrickson, G. H.; Moskovits, M.; Stucky, G. D. *Nature Mater.* **2004**, *3*, 816–822.
(25) Platschek, B.; Petkov, N.; Bein, T. *Angew. Chem., Int. Ed.* **2006**, *45*(7), 1134–1138.
(26) Platschek, B.; Petkov, N.; Himsl, D.; Zimdars, S.; Li, Z.; Köhn, R.; Bein, T. *J. Am. Chem. Soc.* **2008**, *130*(51), 17362–17371.

electrode. A thin copper wire was attached onto the gold film using silver paste. Finally, the electrode side of the composite was carefully isolated against the electrolyte solution using nail polish. Typically, for all the experiments, a volume of 25 mL of the respective electrolyte solution was used for electroplating. The electrolyte solution used for copper deposition was 0.5 M copper sulfate and 0.57 M boric acid. The electrodeposition was performed at various potentials (−0.01 V to −1 V, all potentials are relative to Ag/AgCl) using a three electrode setup and a PAR 2271 potentiostat from Princeton Applied Research. Platinum foil served as counter electrode. A constant flow of nitrogen was bubbled through the electrolyte solution to remove oxygen. The electrodeposition of silver was performed with a two electrode setup from a solution containing 0.5 M $AgNO_3$ and 0.57 M $B(OH)_3$. The deposition potential for Ag was set to 0.01 V using a PAR 2271 potentiostat. A constant flow of nitrogen was bubbled through the electrolyte solution to remove oxygen. Tellurium was electro-deposited from a solution of 1 mmol of TeO_2 and 500 mmol of K_2SO_4 in 100 ml of water. The pH of the electrolyte solution was adjusted to pH 2 by addition of hydrochloric acid to partially dissolve TeO_2.[27,28]

To dissolve selectively only the silica filaments, a small sample was immersed into 2.5 wt % NaOH in a 1:1 mixture of water/ethanol. For a total dissolution of the matrix, a small piece of sample was immersed into 5 wt % NaOH and heated to 60 °C.

Instrumentation. Transmission electron microscopy (TEM) images were recorded using a JEOL JEM 2011 operated at 200 kV and a FEI Titan 80-300 operated at 300 kV. On the latter microscope we also performed energy-dispersive X-ray spectroscopy (EDX) and scanning transmission electron microcopy (STEM). STEM images were recorded in high angle annular dark field (HAADF) mode using a Fischione detector and a camera length of 190 mm.

Results and Discussion

Optimization of the Composite Membrane Synthesis. The general synthesis of mesoporous silica/AAM composites with a hexagonal columnar arrangement of pores has been published recently.[26] As already mentioned in that previous report, the temperature plays a key role during the synthesis of these composites, as high quality hexagonal columnar mesophase systems were only found at an elevated temperature (30 °C). In this work, the synthesis was slightly altered, as the temperature and humidity were precisely controlled and kept constant during the EISA process. The resulting mesophases were evaluated by 2D SAXS (small-angle X-ray scattering) measurements. In a 2D SAXS experiment, the ratio of the hexagonal columnar mesophase to the hexagonal circular mesophase can be estimated by calculating the ratio of the in-plane (ip) reflections (reflections in the horizontal plane of the primary beam) to the out-of-plane (oop) reflections (reflections above or below the horizontal plane).[26] At low humidity (30% r.h.) and in the temperature range examined (27−31 °C), an oop/ip ratio around 1.0 was observed, indicating the presence of the hexagonal circular phase as the predominant phase. At intermediate humidity (50% r.h.) mixed circular and columnar hexagonal phases were found. Well-defined hexagonal columnar mesophases with oop/ip ratios around 0.1 were obtained only at 31 °C and high humidity (70% r.h and higher). The results of this evaluation only yield a trend, as the oop/ip ratios for 27 °C at 70% humidity and the oop/ip ratios for 29 °C and 50% humidity showed strong variations and were not reproducible even on the same membrane. We attribute this behavior to the presence of a phase boundary, where already very small energetic differences have a strong influence on the phase formation.

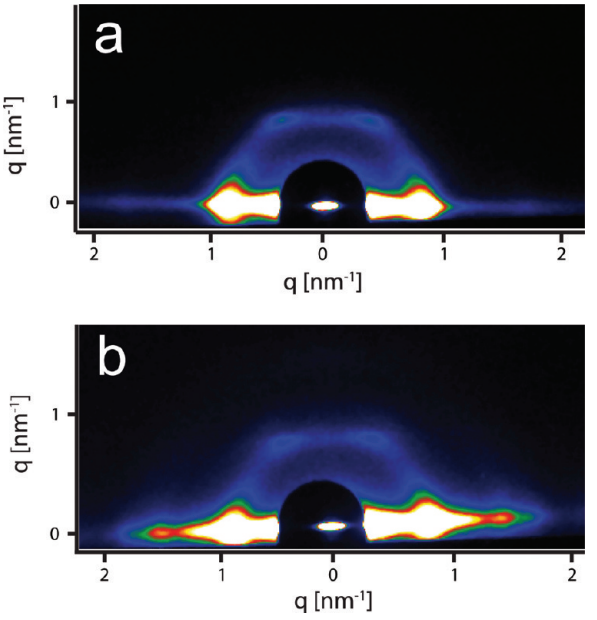

Figure 2. 2D SAXS patterns of a sample synthesized at 31 °C and 70% r.h. before (a) and after calcination (b).

As a result of the above evaluation, we found that an aging temperature over 29 °C and a relative humidity of 75% over at least 12 h yields the highest fraction of the columnar phase. In the SAXS experiment, only very weak reflections characteristic for the hexagonal circular phase could be detected for these experimental conditions. Figure 2 shows typical SAXS patterns as obtained from an as-synthesized sample (a) and a sample calcined at 400 °C (b). The calcined sample shows even stronger reflection intensities than the as-synthesized sample; this result clearly proves that the hexagonal columnar order is perfectly maintained throughout the surfactant removal process.

Structure of the Mesoporous Host and Nanowire Synthesis—Influence of the Electrolyte Concentration and the Deposition Potential. TEM micrographs before electrochemical pore-filling show that not all of the pores are completely filled with the silica mesostructure prior to deposition. In particular, three main defect types have to be considered. First, a few pores of the anodic alumina membrane appear to be unfilled or only partially filled by the mesoporous silica system. Second, the existence of voids between the anodic alumina pore wall and the silica mesostructure has to be taken into account. These defects might be a result of incomplete filling by the precursor sol, or more likely, they could result from pore shrinkage

(27) Lepiller, C.; Cowache, P.; Guillemoles, J. F.; Gibson, N.; Özsan, E.; Lincot, D. *Thin Solid Films* **2000**, *361−362*, 118–122.
(28) Zhao, A.; Zhang, L.; Pang, Y.; Ye, C. *Appl. Phys. A: Mater. Sci. Process.* **2005**, *80*(8), 1725–1728.

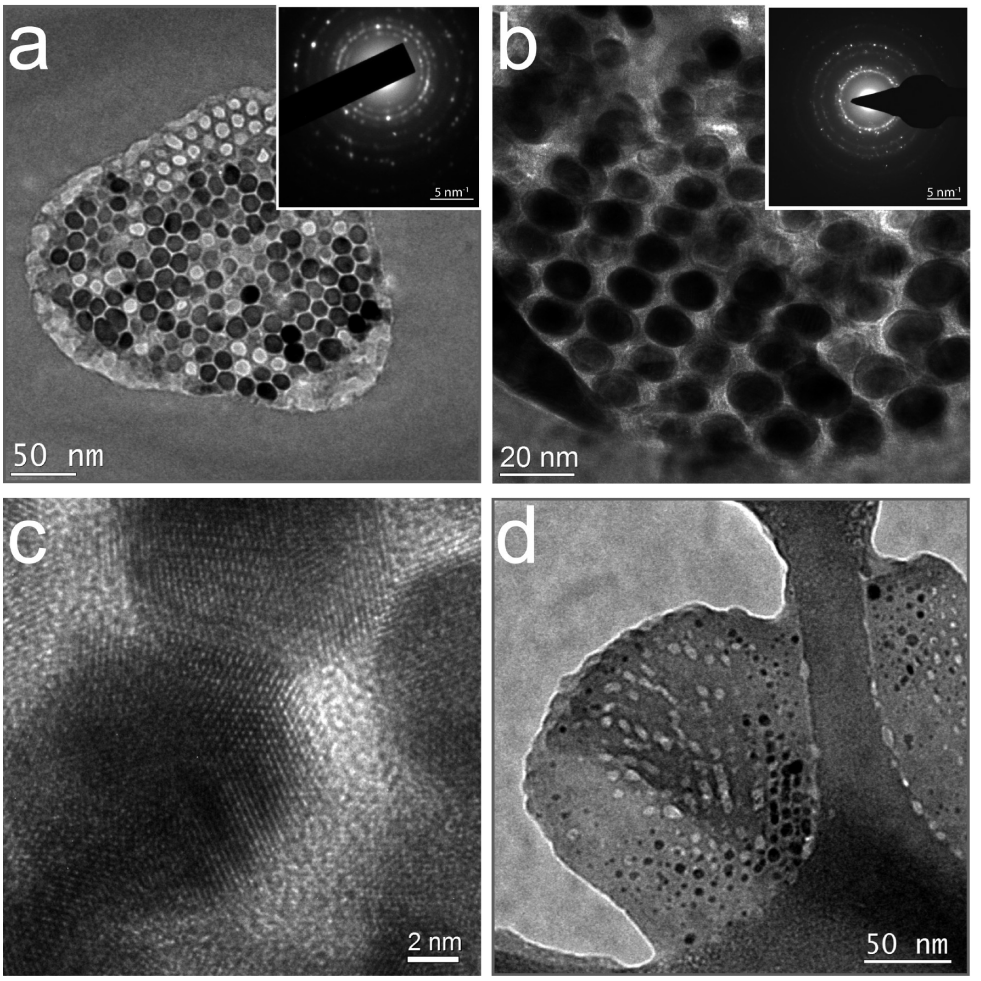

Figure 3. Plan view TEM images of nanowires embedded within the AAM/silica matrix. (a) TEM micrograph of copper nanowires and corresponding electron diffraction pattern (inset). The wire arrangement still perfectly resembles the original hexagonal pattern of the underlying silica mesostructure; the SAED pattern matches that of crystalline copper ($Fm\bar{3}m$). (b) Close-up TEM micrograph of silver nanowires. The inset again shows the SAED pattern of the nanowire structure, which can be indexed according to the crystal structure of elemental silver ($Fm\bar{3}m$). (c) HRTEM of silver nanowires. (d) Tellurium nanowires within the silica structure. The severe distortion of the silica mesophase might result from the rigorous conditions during electrodeposition (see text).

during calcination. Third, due to multipoint nucleation of the silica mesophase in the Anopore channels, one would expect mesophase domain boundaries at fairly large distances in the Anopore membrane; this could cause a few discontinuities in the overall mesopore system along the 60 μm Anopore channels.

For the successful electrodeposition of the wires within the mesoporous system, the concentration of the electrolyte and the deposition potential play an important role. Due to the very high aspect ratio of the pore diameter to the accessible pore length, the rate of diffusion of the ions to the electrode is an important issue. Empty AAM pores or voids in the mesopore/AAM system will show an increased diffusion rate over the small mesopores, while domain boundaries in the silica mesophase can block deposition in certain mesopores. To ensure that the depletion of the ions close to the electrode is slower than the wire growth in adventitious big voids, the concentration of the respective ions must be chosen sufficiently high. Experiments carried out at lower concentrations (0.01−0.1 M) of the respective ions showed almost no filling of the mesoporous system, while a deposition in the empty pores/voids was still observed.

When choosing the correct deposition potential, similar considerations have to be taken into account to enable the deposition in the mesopores. The rate of reduction must be kept low enough to allow simultaneous deposition in the small mesopores and possibly existing voids, cracks, or empty anodic alumina pores. For copper and silver, the same potential of −0.01 V was found to produce optimal results. When choosing more negative deposition potentials, predominant deposition in big voids and/or empty anodic alumina pores was found. When choosing lower potentials, the filling rate of pores decreased and the formation of wires also decreased.

Plan View TEM Micrographs. Plan view images give a good overview over the wire system embedded within the matrix, as both structural aspects and the degree of filling can be visualized. Figure 3 shows plan view TEM micrographs of copper, silver, and tellurium nanowires. The micrographs of copper and silver in Figure 3a−c clearly show the structure characteristic for the original hexagonal columnar order of the silica mesopore system. An estimation of the degree of filling from low magnification images is difficult, as damage of the specimen during sample preparation and the exact location within the

membrane (height) cannot be determined; thus, the degree of pore filling could not be determined quantitatively. To give a more macroscopic impression of this context, low magnification TEM data and an SEM image of a polished sample can be found in the Supporting Information (Figure S5). The images suggest that the filling rate varies over the sample. Furthermore, comparisons between copper-filled and silver-filled samples suggest that higher filling rates can be reached when depositing Cu.

Figure 3a illustrates another interesting aspect that can be derived from plan view images. The thickness of the silica wall material seems to be decreased in areas with filled mesopores, while it is retained in unfilled areas. This might be a result of wire growth, as the crystallization of the electrodeposited metal species apparently exerts enough pressure to compress the amorphous and less dense silica in the mesopore wall.

The average wire diameter is in the range of 10 nm, which is in good agreement with the pore size obtained from sorption measurements (the pore size of the empty Pluronic P123-derived mesopores in AAM membranes is typically in the range 9−11 nm).[26] The micrographs show that there are some deviations in the apparent wire diameter. This might be a result of several effects. First, there might be some wires growing faster than others, expanding the pore size due to crystallization effects and compressing the available pore size in neighboring pores. The wires growing there would then have less space available for growth. The encapsulated wires consist of small connected crystallites, as supported by STEM images of the dissolved wires (discussed below). Second, the pore system might not be perfectly straight, resulting in a small tilt of the tubular system. As TEM images are always projections in the direction of the electron beam, this fact would result in an apparent elongation along one wire axis, also resulting in apparently larger wire diameters. Third, deviations in the shape of the wire might also result in the projection of a larger apparent wire diameter.

The deposition of tellurium proved to be more difficult. The solubility of tellurium oxide in water is very low (10^{-4} M at pH = 2);[27] thus, the growth rate of the tellurium wires is very slow. This results in long deposition times and very poor filling rates. Furthermore, plan view micrographs taken from the synthesized composites (Figure 3d) also show a strong distortion of the silica mesophase itself, which we attribute to the long deposition times (> 12 h) in the highly acidic media.

TEM of Filaments. Plan view micrographs of silica mesophases embedded in an AAM matrix only show a local cross section of the porous system. Thus, the long-range order of the porous system and of the embedded wires cannot be visualized this way. Standard TEM cross sections also suffer from such a drawback, as the electron-transparent area is rather small. Furthermore, these preparation methods involve abrasive steps during specimen preparation (grinding and ion milling). The effect of these steps on the specimen is yet unclear, but we suppose that different milling rates of the ceramic host and the metallic nanowires may lead to changes in morphology. In particular, the degree of filling of the mesopore system with nanowires might be underestimated. Thus, to reveal the long-range order of the silica mesophase and the wires embedded therein, the AAO matrix was selectively dissolved by immersing the samples into a sodium hydroxide solution. This way it was possible to obtain long silica/nanowire composite filaments, whose structure can be studied by TEM.

TEM micrographs of the specimens revealed a large variety of empty, partially filled, and completely filled silica filaments. Here we focus on the imaging of partially filled filaments, because completely filled filaments tend to become intransparent for electrons due to their projected thickness of up to 300 nm. Micrographs of partially filled filaments (Figure 4) give an overview on the structural diversity of filaments. As already discussed above for the plan view images, the hexagonal arrangement of the original mesopore system is perfectly replicated. The average wire diameter is again in the range of 10 nm. The hexagonal columnar phase is the dominant phase; however, orientational switching of the hexagonal phase between the columnar and the circular orientations of the hexagonal channel system can be observed in some regions over the whole length of the filaments. Wires grown in regions exhibiting the hexagonal columnar phase (Figure 4a) illustrate that the porous system can be twisted in such regions, while leaving the hexagonal short-range order intact. This cannot be readily visualized with thin sliced plan view samples. In regions exhibiting the hexagonal circular phase (Figure 4b) similar geometries as for plan view images can be observed, as expected. Many of the silica filaments show phase boundaries from one phase orientation to another, with the wires following these structures (Figure 4c).

Another interesting feature is the existence of larger chunks attached to the sides of some filaments as depicted in Figure 4d. These metal objects are attributed to defect sites in the Anopore channels that had not been completely filled by mesoporous silica but could still be filled with metal through diffusion from neighboring mesopores.

By stitching together a series of images ("mapping"), the long-range arrangements in such filaments can be visualized over several micrometers (see Supporting Information, Figure S7).

TEM of Free-Standing Wires. Free silver nanowires could be obtained by dissolving the host matrix completely in a hot sodium hydroxide solution (TEM and STEM micrographs in Figure 5). Dissolution experiments carried out at room temperature resulted only in the dissolution of the alumina membrane, while the silica/metal filaments stayed intact.

The free-standing wires vary in length; most of the wires appear to be broken either during preparation for TEM or directly during the dissolution process (Figure 5a). Due to the nature of electrochemical growth with the wire tip always acting as the active cathode for further wire growth,

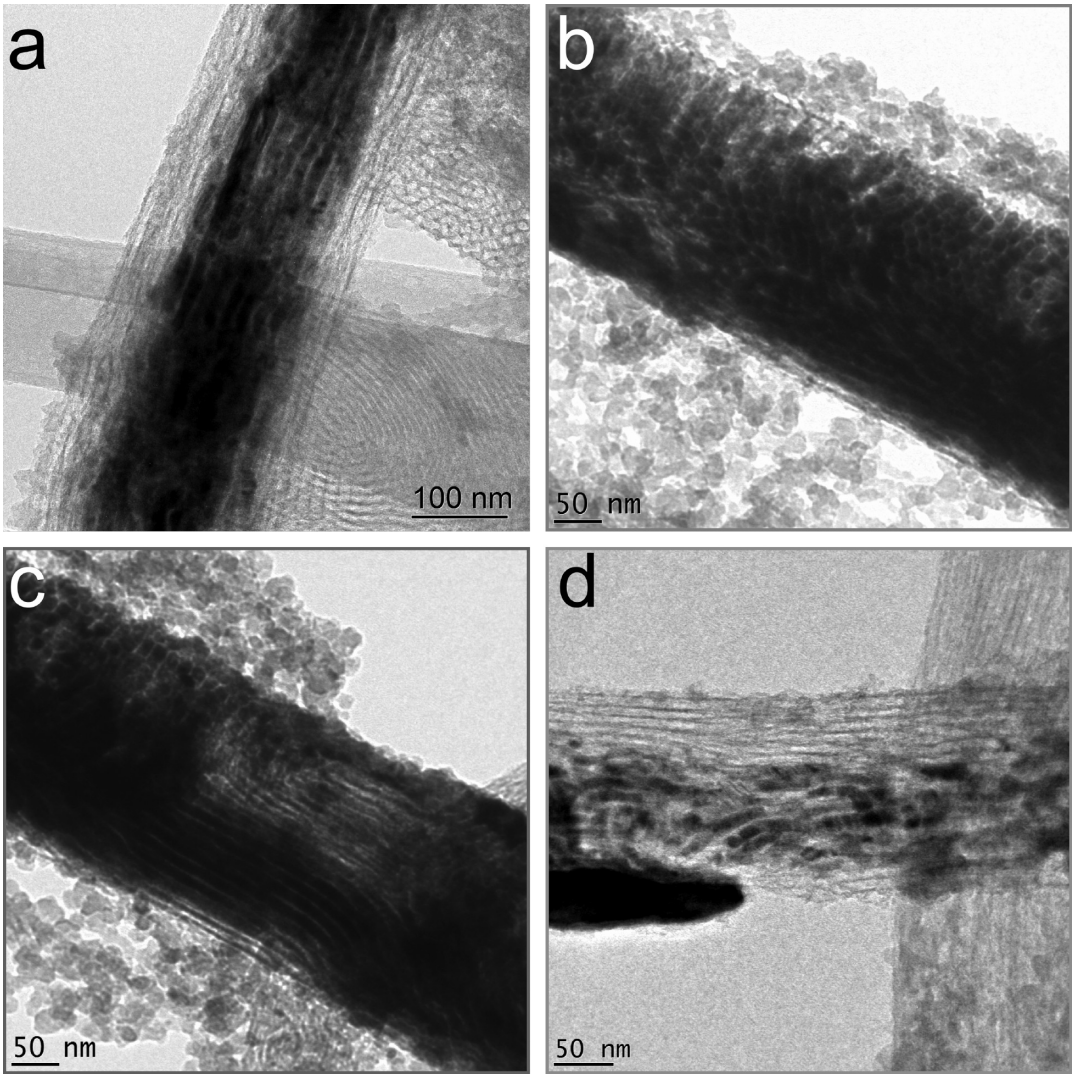

Figure 4. TEM micrographs of silica filaments dissolved from the AAM mold and filled with copper nanowires. (a) Silica filament filled with columnar nanowires. (b) Filament with the hexagonal circular mesostructure. The wires still follow the circular host structure. (c) TEM micrograph of a phase-change region. The mesosystem orientation changes from a columnar to a circular domain. (d) Filament with a copper chunk.

all broken wire fragments must have been connected during growth and as long as they were still embedded within the silica matrix. In micrographs obtained from the isolated silica filaments (Figure 4), no evidence for broken wires could be found. We note that no coiled wires could be found that would have resulted from the hexagonal circular mesostructure, which implies either that these wires have uncoiled or that the fraction of the circular mesophase was negligible. The average wire diameter determined from the micrographs is still within the range of 10 nm.

HRTEM micrographs as depicted in Figure 5b did not show any direct evidence for the presence of interwire connects resulting from deposition within the microporous pore walls of the silica phase. However, the wires were always found to be agglomerated to bundles; Ryoo et al. have attributed the existence of such bundles to the presence of micropore interconnects,[29] gluing together individual wires even after removal of the silica mold. The indexing of the SAED patterns in the inset of Figure 5a reveals the formation of the standard cubic ($Fm\bar{3}m$) silver phase (Figure S8). This also corresponds to wide-angle X-ray diffraction data obtained from the respective membranes. STEM-HAADF images show that the individual wires exhibit slight variations in their contrast (Figure 5c), which could be due to variations in thickness.

The complete dissolution of the host matrix could be clearly proven by EDX measurements. The spectra depicted in Figure 5d show strong signals for silver but no signals for the elements of the double mold matrix (aluminum and silicon). The signals for copper result from the copper grid used as a substrate for electron microscopy. The presence of only traces of oxygen indicates that the wires have not been oxidized to silver oxide, which is confirmed by SAED diffraction (inset in Figure 5a).

In contrast to the case of silver nanowires, free copper nanowires could not be successfully prepared by the described approach. TEM micrographs taken from such

(29) Ryoo, R.; Ko, C. H.; Kruk, M.; Antochshuk, V.; Jaroniec, M. *J. Phys. Chem. B* **2000**, *104*(48), 11465–11471.

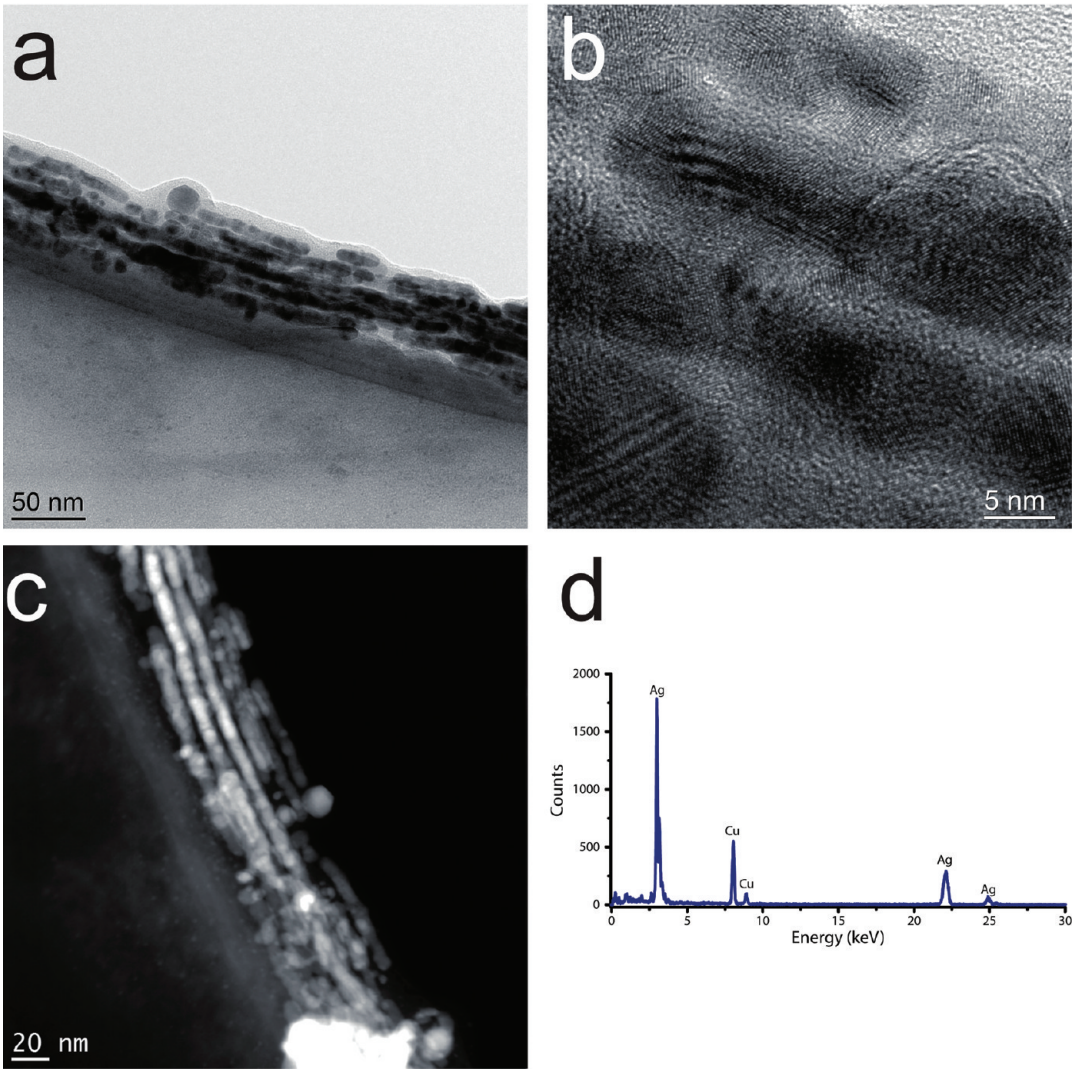

Figure 5. Characterization of the isolated silver wires. (a) TEM micrograph of isolated Ag wires adhered to the carbon support of a TEM grid. The inset shows the SAED pattern obtained from the wires. The pattern can be indexed to the standard ($Fm\bar{3}m$) silver phase. (b) HRTEM micrograph of the wires, illustrating the polycrystalline nature of the wires. (c) HAADF STEM image of the isolated silver wires. (d) EDX data proving the complete absence of the mold composite material (AAM/silica matrix). The low oxygen content also indicates that the wires have not been oxidized during the mold removal process. The copper signals result from the supporting copper grid in TEM.

samples only showed formation of large amounts of salts, as copper apparently does not withstand the treatment with hot NaOH.

Conclusion

In summary, we have successfully synthesized copper and silver nanowires with diameters of approximately 10 nm by electrochemistry within hierarchical mesoporous composite structures. The existence of these wires within the matrix was demonstrated with plan view TEM, STEM, and EDX measurements. TEM micrographs of free silica filaments filled with copper show that the metal phase can replicate the mesoporous phase over a long distance (>1 μm). Individual silver nanowires could be completely dissolved from the matrix.

The plan view micrographs of both the silver and the copper nanowires embedded in the mesoporous composite matrix show an almost perfect hexagonal alignment originating from the host silica mesophase. TEM-maps generated from micrographs of isolated silica filaments filled with copper provide insights into the domain structure of the Anopore-embedded mesoporous silica; an orientational switching between columnar and circular hexagonal phases can be observed. Finally, silver nanowires could be completely isolated from the host matrix, as proven by TEM, STEM, and EDX measurements.

Acknowledgment. The authors gratefully acknowledge funding for this work from the Deutsche Forschungsgemeinschaft through the SFB 486 and the Nanosystems Initiative Munich (NIM Cluster). J.M. thanks the RISE program of the DAAD (Deutscher Akademischer Auslandsdienst) and the Center for Nanoscience (CeNS) for financial support.

Supporting Information Available: SAED patterns, HR-TEM image, EDX spectrum, SEM image, and TEM image. This material is available free of charge via the Internet at http://pubs.acs.org.